INTERNATIONAL JOURNAL FOR NUMERICAL METHODS IN FLUIDS, VOL. 21, 141–153 (1995)

DAMPED ARTIFICIAL COMPRESSIBILITY ITERATION SCHEME FOR IMPLICIT CALCULATIONS OF UNSTEADY INCOMPRESSIBLE FLOW

P. R. McHUGH AND J. D. RAMSHAW

Idaho National Engineering Laboratory, P. O. Box 1625, Idaho Falls, ID 83415-3808, U.S.A.

SUMMARY

Peyret (*J. Fluid Mech.*, **78**, 49–63 (1976)) and others have described artificial compressibility iteration schemes for solving implicit time discretizations of the unsteady incompressible Navier–Stokes equations. Such schemes solve the implicit equations by introducing derivatives with respect to a pseudo-time variable τ and marching out to a steady state in τ. The pseudo-time evolution equation for the pressure p takes the form $\partial p/\partial \tau = -a^2 \nabla \cdot \mathbf{u}$, where a is an artificial compressibility parameter and $\mathbf{u}$ is the fluid velocity vector. We present a new scheme of this type in which convergence is accelerated by a new procedure for setting a and by introducing an artificial bulk viscosity b into the momentum equation. This scheme is used to solve the non-linear equations resulting from a fully implicit time differencing scheme for unsteady incompressible flow. We find that the best values of a and b are generally quite different from those in the analogous scheme for steady flow (J. D. Ramshaw and V. A. Mousseau, *Comput. Fluids*, **18**, 361–367 (1990)), owing to the previously unrecognized fact that the character of the system is profoundly altered by the presence of the physical time derivative terms. In particular, a Fourier dispersion analysis shows that a no longer has the significance of a wave speed for finite values of the physical time step Δt. Indeed, if one sets $a \sim |\mathbf{u}|$ as usual, the artificial sound waves cease to exist when Δt is small and this adversely affects the iteration convergence rate. Approximate analytical expressions for a and b are proposed and the benefits of their use relative to the conventional values $a \sim |\mathbf{u}|$ and $b = 0$ are illustrated in simple test calculations.

KEY WORDS: incompressible flow; artificial compressibility; artificial bulk viscosity

1. INTRODUCTION

The artificial compressibility (AC) method[1–5] is widely used for solving the steady state incompressible Navier–Stokes equations. In this method the steady solution is computed as the asymptotic limit of an artificial transient process in a pseudo-time variable τ. Compressibility is artificially introduced by setting

$$\frac{\partial p}{\partial \tau} = -a^2 \nabla \cdot \mathbf{u} \tag{1}$$

where p is the pressure (divided by density), $\mathbf{u}$ is the fluid velocity vector and a is an artificial sound speed. One ordinarily sets $a \sim |\mathbf{u}|$ so that convective and acoustic effects occur on similar time scales. Equation (1) and the momentum equation are simultaneously marched out in τ until a steady solution is obtained. The incompressibility condition $\nabla \cdot \mathbf{u} = 0$ is artificially violated during the artificial transient but is satisfied in steady state when $\partial p/\partial \tau = 0$. The continuing popularity of the AC method is due in large part to its simplicity and clear physical interpretation.

CCC 0271–2091/95/020141–13

Received 24 May 1994
Revised 24 October 1994

The equations resulting from implicit time discretizations of the unsteady incompressible Navier–Stokes equations are similar in structure to the steady state equations. The incompressibility condition is unchanged and the fully implicit unsteady momentum equation is obtained simply by adding a backward time derivative of velocity to the corresponding steady equation. These implicit equations should therefore be amenable to solution by time-like AC iteration schemes similar to the steady state AC method. Schemes of this type have indeed been described and applied by Peyret[6,7] and others.[8–10]

It has recently been shown that convergence of the steady state AC method can be significantly accelerated by introducing an artificial bulk viscosity b to remove the artificial sound waves more rapidly.[11] The original purpose of the present work was to investigate whether AC iteration schemes for implicit unsteady calculations can be accelerated in a similar way. In doing so, however, we encountered some unexpected and counter-intuitive behaviour. In particular, we observed that for small values of the physical time step Δt, convergence could be greatly accelerated by letting a be much larger than conventional values of order $|\mathbf{u}|$, in spite of the fact that this required a corresponding reduction in the pseudo-time step $\Delta\tau$. Moreover, when this was done, we obtained no benefits from b. For sufficiently large Δt, however, conventional values of a again worked best and the use of b again produced benefits similar to those previously obtained in the steady state case.[11]

These observations led us to examine the character of the pseudo-time evolution equations using Fourier dispersion analysis. This analysis showed that the physical time derivative term in the momentum equation introduces additional damping which can profoundly alter the character and behaviour of the system. This damping is proportional to $1/\Delta t$, so it becomes very large for small Δt. There is then no need to supply any additional damping, which explains why b was not found to be beneficial in this regime. The analysis further shows that the parameter a no longer has the interpretation of a wave speed for finite Δt. Indeed, for small enough Δt and conventional values of $a \sim |\mathbf{u}|$ the system becomes overdamped and the artificial sound waves cease to exist! The system then loses its hyperbolic behaviour and becomes purely parabolic or diffusional. However, the waves are restored by using the larger values of a that were observed to result in accelerated convergence. Thus it appears that the artificial sound waves play an essential role in obtaining rapid convergence. This is in accordance with the growing evidence that combinations of hyperbolic and parabolic behaviour often produce faster convergence than either one alone.[11–13] The beneficial effects of the artificial sound waves are also confirmed by a Fourier convergence rate analysis[14–16] of the simplified equations with convection terms omitted.

Guided by these insights, we proceeded to postulate that the *actual* artificial sound speed c rather than the parameter a should be set to a value of order $|\mathbf{u}|$ and that the total rate at which long wavelengths are damped by *both* Δt and b should be similar to that at which they are damped by b alone in steady state calculations ($\Delta t \to \infty$). We thereby obtained simple approximate analytical expressions for a and b containing corresponding dimensionless coefficients α and β of order unity. These expressions provide reasonable first estimates of a and b which usually produce iteration counts within about 25% of the best values found empirically by numerical experiments.

The paper is organized as follows. In Section 2 we define the fully implicit time differencing scheme that we use to generate approximate numerical solutions to the unsteady incompressible Navier–Stokes equations. This scheme produces a system of coupled non-linear algebraic equations for the pressure and fluid velocity at the advanced time level. We then present the damped artificial compressibility iteration scheme that we use to solve this system, together with the associated stability restrictions on the pseudo-time step $\Delta\tau$. In Section 3 we analyse the behaviour of the iteration scheme by means of a long-wavelength Fourier dispersion analysis. This analysis yields information about wave speed, damping and convergence rate. Based on these results, we propose expressions for the parameters a and b as discussed above. In Section 4 we apply the scheme to the solution of two test problems, a driven cavity and flow past a rectangular obstacle, for several different spatial discretizations and

values of Δt. The resulting iteration counts are compared with those resulting from the conventional values $a \sim |\mathbf{u}|$ and/or $b = 0$. Finally, a few concluding remarks are given in Section 5.

2. TIME DIFFERENCING AND ITERATION SCHEME

Our overall objective is to develop a suitable scheme for obtaining approximate numerical solutions of the unsteady incompressible Navier–Stokes equations

$$\nabla \cdot \mathbf{u} = 0 \tag{2}$$

$$\frac{\partial \mathbf{u}}{\partial t} + \mathbf{u} \cdot \nabla \mathbf{u} = -\nabla p + \nu \nabla^2 \mathbf{u}, \tag{3}$$

where ν is the kinematic viscosity. The numerical solution will be obtained at a sequence of discrete times $t^n (n = 0, 1, 2, \ldots)$ separated by time increments or time steps $\Delta t = t^{n+1} - t^n$. As usual, time levels will be displayed as superscripts, so that Q^n denotes the approximation to the quantity Q at time $t = t^n$. We shall adopt a fully implicit temporal differencing scheme in which time derivatives are approximated by backward differences and all other quantities are evaluated at the advanced time level. We thereby obtain

$$\nabla \cdot \mathbf{u}^{n+1} = 0, \tag{4}$$

$$\frac{\mathbf{u}^{n+1} - \mathbf{u}^n}{\Delta t} + (\mathbf{u} \cdot \nabla \mathbf{u})^{n+1} = -\nabla p^{n+1} + \nu \nabla^2 \mathbf{u}^{n+1} \tag{5}$$

Partially implicit schemes, such as Crank–Nicolson, and linearly implicit schemes, in which the convective terms are linearized in $\mathbf{u}^{n+1}$, are also commonly employed. We prefer the fully implicit scheme for several reasons: (i) The fully implicit scheme provides the option of calculating steady state solutions in a single time step simply by setting Δt to a very large value. (ii) Crank–Nicolson differencing of the viscous terms, while second-order-accurate and unconditionally stable, is known to produce irregular solutions for very large Δt,[17] whereas the fully implicit scheme produces qualitatively reasonable solutions for any Δt, however large. (iii) A Crank–Nicolson treatment of the pressure gradient term alone has no significant effect: it yields the same velocity field as the simpler fully implicit treatment. To see this, consider the effect of replacing p^{n+1} by a scalar potential ϕ in (5). Equations (4) and (5) then determine a unique solution for $\mathbf{u}^{n+1}$ and ϕ regardless of whether we subsequently interpret ϕ as p^{n+1} or $(p^n + p^{n+1})/2$. Thus the Crank–Nicolson value of $(p^n + p^{n+1})/2$ is identical with the fully implicit value of p^{n+1}, so the only difference between the two treatments is a slight difference in the time dependence of the pressure field.

The spatial derivatives in (4) and (5) are of course also approximated by a suitable spatial discretization scheme and this will be understood in what follows. The present method should be compatible with any reasonably well-behaved spatial discretization scheme, including finite element and spectral schemes as well as finite differences. (The detailed convergence behaviour, however, may well depend to some degree on the particular spatial scheme that is used.) In the present study, spatial derivatives were approximated by simple low-order finite difference approximations on a uniform two-dimensional rectangular mesh with spatial increments Δx and Δy. We used a conventional staggered scheme based on the MAC placement of variables[7] in which pressures are located at cell centres while normal velocity components are located on cell faces. Centred spatial differencing was used for all terms except convection, which was represented by upwind or donor cell differencing for simplicity.

Equations (4) and (5) constitute a system of non-linear algebraic equations for the quantities $\mathbf{u}^{n+1}$ and p^{n+1} at each mesh point. This system must be solved in order to advance the solution from one

time level to the next. This is done by means of a time-like iteration scheme which may be written in differential form as

$$\frac{\partial p}{\partial \tau} = -a^2 \nabla \cdot \mathbf{u}, \tag{6}$$

$$\frac{\partial \mathbf{u}}{\partial \tau} = -\frac{\mathbf{u} - \mathbf{u}^n}{\Delta t} - (\mathbf{u} \cdot \nabla \mathbf{u}) - \nabla(p - b\nabla \cdot \mathbf{u}) + \nu \nabla^2 \mathbf{u}, \tag{7}$$

where τ is an artificial pseudo-time variable and $b > 0$ is an artificial bulk viscosity. These equations are to be marched out to a steady state in pseudo-time. The derivatives $\partial/\partial\tau$ then vanish and comparison with (4) and (5) shows that p and $\mathbf{u}$ then converge to the advanced time values p^{n+1} and $\mathbf{u}^{n+1}$. The essential new feature of the present scheme is the artificial bulk viscosity term in (7). Previous schemes of this type[6–10] are essentially all based on various numerical implementations of (6) and (7) with $b = 0$.

Equations (6) and (7) are solved numerically by discretizing τ and approximating the pseudo-time derivatives as finite differences over pseudo-time increments $\Delta\tau$. The pseudo-time level i is equivalent to an iteration index and will be displayed as a superscript in parentheses. We use a simple fully explicit pseudo-time differencing scheme which is well suited to vector and parallel processing. This scheme is given by

$$\frac{p^{(i+1)} - p^{(i)}}{\Delta \tau} = -a^2 \nabla \cdot \mathbf{u}^{(i)}, \tag{8}$$

$$\frac{\mathbf{u}^{(i+1)} - \mathbf{u}^{(i)}}{\Delta \tau} = -\frac{\mathbf{u}^{(i)} - \mathbf{u}^n}{\Delta t} - (\mathbf{u} \cdot \nabla \mathbf{u})^{(i)} - \nabla(p^{(i+1)} - b\nabla \cdot \mathbf{u}^{(i)}) + \nu \nabla^2 \mathbf{u}^{(i)}. \tag{9}$$

One might at first think that it would be advantageous to evaluate $\mathbf{u}$ in the Δt term as $\mathbf{u}^{(i+1)}$ rather than $\mathbf{u}^{(i)}$, since this would still allow an explicit solution for $\mathbf{u}^{(i+1)}$. However, this would be an illusory modification, since it is algebraically equivalent to simply redefining the parameters $\Delta\tau$ and a.

Equations (8) and (9) define the iteration scheme used to solve the non-linear algebraic system of equations (4) and (5). The free parameters a and b are at our disposal. They should of course be set to values that maximize the rate of convergence, as discussed in Section 3 below.

The pseudo-time increment $\Delta\tau$ is restricted by the applicable explicit stability limit, which may be approximately determined by a linearized Fourier or von Neumann analysis in the usual way.[7] The detailed form of this stability restriction depends on the details of the spatial differencing and this may in turn affect the convergence rate to some degree. However, we would expect this effect to be relatively minor, since different spatial schemes tend to have similar stability limits for the same time differencing. Different spatial schemes will also differ in their artificial or numerical viscosities and this may have some effect on the optimal value of the artificial bulk viscosity b. In particular, the use of convective schemes with smaller artificial viscosities may well shift the optimal b to somewhat larger values than those found in the present study. Thus the use of alternative spatial difference schemes may have some effect on the optimal values of a and b, but this effect seems unlikely to be dramatic.

We now proceed to determine a suitable approximation to the stability restriction on $\Delta\tau$ for the present scheme. For simplicity we shall consider the stability of the convective terms separately from that of the remaining terms. The overall stability condition will then be approximated by the more restrictive of the resulting separate stability conditions. The convective stability limit for upwind differencing in a rectangular mesh is well known and is given by $\Delta\tau < \Delta\tau_c$, where

$$\Delta\tau_c = \min \left(\frac{|u|}{\Delta x} + \frac{|v|}{\Delta y} \right)^{-1}. \tag{10}$$

Here u and v are the x- and y-components of $\mathbf{u}$ respectively and the minimum is taken over all cells in the computing mesh.

We now consider the stability of the scheme with the convection terms omitted. For this purpose it is convenient to consider the velocity divergence $\nabla \cdot \mathbf{u}$ and the vorticity $\nabla \times \mathbf{u}$ separately, since the former is directly coupled to the pressure whereas the latter is not. The divergence of (9) may be combined with (8) to obtain an equation for p or $\nabla \cdot \mathbf{u}$ alone. A Fourier analysis of the result yields the stability condition $\Delta\tau < \Delta\tau_d$, where $\Delta\tau_d$ is determined by

$$\frac{a^2\Delta\tau_d^2}{\Delta^2} + \frac{2(b+v)\Delta\tau_d}{\Delta^2} + \frac{\Delta\tau_d}{2\Delta t} = 1, \tag{11}$$

with $\Delta^2 = (1/\Delta x^2 + 1/\Delta y^2)^{-1}$. Solving for $\Delta\tau_d$, we obtain

$$\Delta\tau_d = \frac{1}{2A}\left[-B + \sqrt{(B^2 + 4A)}\right], \tag{12}$$

where $A = a^2/\Delta^2$ and $B = 2(b+v)/\Delta^2 + 1/2\Delta t$.

The vorticity equation is obtained by taking the curl of (9). The pressure term then drops out, so the resulting equation involves the vorticity alone. A Fourier analysis of this equation yields a stability condition which is always less restrictive than the previous one and may therefore be ignored.

The overall stability condition is now approximated by $\Delta\tau < \min(\Delta\tau_c, \Delta\tau_d)$ or, equivalently,

$$\Delta\tau = f \min(\Delta\tau_c, \Delta\tau_d), \tag{13}$$

where f is a safety factor between zero and unity.

The scheme of equations (8) and (9) must be initialized by specifying values for $p^{(0)}$ and $\mathbf{u}^{(0)}$, which should of course represent one's best estimate of the final converged solution. There are at least three obvious initializations that might be considered, namely

(a) $(p, \mathbf{u})^{(0)} = (p, \mathbf{u})^n$ (previous time level)
(b) $(p, \mathbf{u})^{(0)} = 2(p, \mathbf{u})^n - (p, \mathbf{u})^{n-1}$ (extrapolation)
(c) explicit predictor

where (c) is obtained by setting $\Delta\tau = \Delta t$ on the first iteration of (a). Which of these initializations is best will be problem-dependent and will depend upon Δt as well as on whether the flow is evolving rapidly or slowly. In the present study we have restricted attention to initialization (a) and have not systematically explored the use of (b) or (c).

The solution is then marched out in pseudo-time or i until it converges to a steady state as $i \to \infty$. Of course, the solution is converged for all practical purposes at some finite (and hopefully small) value of i, at which point the iteration may be terminated. This point is determined by an appropriate convergence criterion. We consider the iteration to be converged when both the following conditions are satisfied:

$$|\nabla \cdot \mathbf{u}| < \varepsilon_d \frac{U}{L_d}, \tag{14}$$

$$\left|\frac{\omega^{(i+1)} - \omega^{(i)}}{\Delta\tau}\right| < \varepsilon_v \left(\frac{U}{L_d}\right)^2, \tag{15}$$

where $\omega = \nabla \times \mathbf{u}$ is the vorticity, U is the maximum value of $\sqrt{(u^2 + v^2)}$ anywhere in the computing mesh or on the boundaries, $L_d = \sqrt{(L_x^2 + L_y^2)}$, L_x and L_y are characteristic lengths in the x- and y-directions respectively and ε_d and ε_v are dimensionless tolerances. We currently set $\varepsilon_d = 10^{-5}$ and

$\varepsilon_v = 10^{-2}$, which are small enough that the solution is not sensibly changed by reducing them further in test calculations.

3. FOURIER DISPERSION AND CONVERGENCE ANALYSIS

We now proceed to analyse the behaviour of the iteration scheme at long wavelengths by means of a linearized Fourier dispersion analysis. For long wavelengths the differential equations (6) and (7) are very accurate approximations to the discrete equations (8) and (9). We may therefore simply perform a *differential* Fourier dispersion analysis of (6) and (7), which significantly simplifies the algebra. The purpose of the analysis is to obtain insight into the wave propagation and damping characteristics of the scheme in the simplest possible setting. To this end we remove inessential complications by adopting two further simplifications: (i) The convection terms will be neglected. The equations then become linear and no further linearization is needed. (ii) We specialize to the case of one-dimensional flow in the x-direction.

We seek solutions in which the dependent variables are Fourier modes of the form $p = \hat{p}\exp[i(kx - \omega t)]$ and $u = \hat{u}\exp[i(kx - \omega t)]$, where k is the wave number and ω is the angular frequency. The wavelength corresponding to k is $\lambda = 2\pi/k$, which must be much larger than Δx for the continuous analysis to apply. The longest meaningful wavelength in a computational region of length L is $\lambda = 2L$, which corresponds to a wave number $k = k_L \equiv \pi/L$. Substituting these Fourier modes into (6) and (7), we find that non-trivial solutions exist only when ω and k are related by the dispersion relation

$$\frac{\omega}{k} = -ia_0 \pm \sqrt{(a^2 - a_0^2)}, \tag{16}$$

where a_0 is a critical value of a given by

$$a_0 = \frac{1}{2}\left(\frac{1}{k\Delta t} + (b + v)k\right). \tag{17}$$

The imaginary part of ω determines the rate of growth or decay of the Fourier mode, while the real part of ω/k determines the wave speed c. The wave speed therefore vanishes for $a < a_0$ and is given by

$$c = \sqrt{(a^2 - a_0^2)} \tag{18}$$

for $a > a_0$. Thus c is always less than a, becoming smaller for larger a_0. Since a_0 depends on k, so does c and the system is dispersive.

The present analysis is restricted to long wavelengths (i.e. small k), for which the viscous terms in (17) are small. The magnitude of a_0 is therefore primarily governed by the Δt term in (17). When Δt is large, a_0 is small and $c \approx a$, which is of course the usual interpretation of a. For smaller Δt, however, a_0 becomes larger and this interpretation is no longer valid. Indeed, for given values of a and k there is a critical value of Δt below which a_0 exceeds a and the artificial sound waves cease to exist. This intuitively seems undesirable, since there is growing evidence that combinations of wave-like and diffusional behaviour exhibit better convergence properties than either one alone.[11–13] In order to preserve the artificial sound waves for a given k, it is necessary to increase a as Δt is reduced so that a remains greater than a_0. This requires larger values of a for smaller k, since the dominant term in a_0 is inversely proportional to k. Thus a_0 is largest and c is smallest when k is smallest, i.e. for $k = k_L = \pi/L$. The resulting maximum a_0 is given by

$$a_L = \frac{1}{2}\left(\frac{1}{k_L\Delta t} + (b + v)k_L\right). \tag{19}$$

Values of a larger than a_L therefore preserve the artificial sound waves for all wavelengths. However, these larger values of a require smaller values of $\Delta\tau$ for stability and one might intuitively suspect that this would reduce the convergence rate, thereby negating any benefits the waves might otherwise provide. Perhaps surprisingly, however, this does not occur. Both numerical experiments and a heuristic Fourier convergence rate analysis (see below) show that the fastest convergence is in fact obtained by setting $a > a_L$, in spite of the resulting reduction in $\Delta\tau$.

The heuristic convergence rate analysis[14–16] is based on the fact that the overall rate of convergence is typically limited by the Fourier modes with $k = k_L$, for which

$$\omega = k_L\left[-ia_L \pm \sqrt{(a^2 - a_L^2)}\right]. \tag{20}$$

The amplitude of these modes decays by a factor $\exp[\Delta\tau \mathrm{Im}(\omega)]$ on each iteration. The convergence rate R is defined by equating this factor to $\exp(-R)$ so that

$$R = -\Delta\tau \mathrm{Im}(\omega). \tag{21}$$

Since there are two roots for ω according to (20), there are two corresponding values for R and the overall convergence rate is the smaller of these two values.[16] Combining (20) and (21) with this in mind, we obtain

$$R = fk_L\Delta\tau_d \begin{cases} a_L & (a > a_L), \\ a_L - \sqrt{(a_L^2 - a^2)} & (a < a_L), \end{cases} \tag{22}$$

where use has been made of the fact that $\Delta\tau = f\Delta\tau_d$ in the absence of convection. The factor $\Delta\tau_d$ of course depends on a and b via (12). We now wish to find the values of a and b which produce the largest R. First we shall maximize R with respect to a at fixed b. To this end we consider $\partial R/\partial a$, which may be shown to be positive for $a < a_L$ and negative for $a > a_L$. The maximum R is therefore attained for $a = a_L$, which is just the critical value which a must exceed for waves to exist! Setting $a = a_L$, we then have $R = fa_L\Delta\tau_d$, which still depends on b through a_L and $\Delta\tau_d$. The next step is to maximize this expression with respect to b. We find that $\partial R/\partial b < 0$, so the maximum R is obtained by using the smallest allowed value of b, namely $b = 0$. Thus the optimal parameter values in the case of no convection are $a = a_L$ and $b = 0$. Even when convection is present, we may anticipate that these values will be nearly optimal for very small Δt. In this case a_L becomes very large, so that $|\mathbf{u}| \ll a$. Convection is then a much slower process than wave propagation and its effect on the convergence rate should correspondingly be small.

When $a \geqslant a_0$, we find from (16) and (17) that

$$-\mathrm{Im}(\omega) = \frac{1}{2}\left(\frac{1}{\Delta t} + (b + \nu)k^2\right), \tag{23}$$

which is a characteristic damping rate in pseudo-time. This rate is seen to be the sum of a term proportional to $1/\Delta t$ and a term proportional to k^2. The k^2 term represents viscous damping, which is large for short wavelengths but small for long ones, while the $1/\Delta t$ term damps all wavelengths at a uniform rate that becomes large for small Δt. This latter damping is due to the physical time derivative term in (7). If the other terms were absent, this term would simply produce an exponential relaxation of $\mathbf{u}$ to $\mathbf{u}^n$ with a pseudo-time constant of Δt. Owing to its wavelength independence, this type of damping is actually preferable to viscous damping. When this term is significant, the additional damping provided by b is evidently not needed and indeed becomes undesirable, since it requires an unnecessary reduction in $\Delta\tau$. As discussed above, when Δt is small, we would expect a similar situation even with convection present.

Guided by these insights, we shall rely on heuristic arguments to propose values for a and b suitable for general use when convection is present and Δt is arbitrary. All indications are that artificial sound

waves are desirable and should be preserved, which we shall ensure by requiring that $a > a_L$. We further postulate that the speed of these artificial waves at long wavelengths should be of order $|\mathbf{u}|$ so that convective and acoustic effects occur on similar time scales, just as in the original AC method.[1] According to (18), the wave speed at long wavelengths is given by $c_L = \sqrt{(a^2 - a_L^2)}$. There is some ambiguity in setting $c_L \sim |\mathbf{u}|$, not merely in the choice of a proportionality constant but also because $\mathbf{u}$ generally depends on space and time. In some situations, particularly in non-uniform meshes with large spatial variations in Δ, it may be advantageous to also allow c_L to vary in both space and time. In the present study, however, we simply set $c_L \sim U$ so that $a^2 \sim a_L^2 + U^2$ or

$$a^2 = \alpha^2(a_L^2 + U^2), \tag{24}$$

where α is a dimensionless coefficient of order unity. In the case of no convection, where $\mathbf{u} = 0$, this properly reduces to $a \sim a_L$.

We now consider how to set b. According to (23), the damping rate for $k = k_L$ at finite Δt may be regarded as resulting from a net *effective* viscosity $\nu_e = b + \nu + 1/k_L^2 \Delta t$. This suggests that the convergence rate is likely to depend more simply on ν_e than on b itself, which leads us to hypothesize that in contrast with b, the best value of ν_e may be relatively independent of Δt. If so, the best value of ν_e will be close to that of $b + \nu$ in steady state calculations ($\Delta t \to \infty$), which is known to be of order $U\Delta$.[11] We are therefore led to postulate that ν_e should be proportional to $U\Delta$, subject of course to the restriction that $b > 0$. We thereby obtain

$$b = \max\left(0,\ \beta U\Delta - \nu - \frac{1}{k_L^2 \Delta t}\right), \tag{25}$$

where β is a dimensionless coefficient of order unity.

The above considerations are still restricted to the case of one spatial dimension. In the two-dimensional case we evaluate k_L in (19) and (25) as $\sqrt{(k_X^2 + k_Y^2)}$, where $k_X = \pi/L_x$ and $k_Y = \pi/L_y$.

The damping rate at long wavelengths is also influenced to some degree by the artificial viscosity of the numerical scheme, which has been neglected in the present development. It might be possible to obtain a more accurate expression for b by taking this effect into account, especially in schemes with large artificial viscosities, but we have not explored this possibility.

The overall procedure for setting the parameters is therefore as follows. One first determines b using (25). The result combines with (19) to determine a_L, which then combines with (24) to determine a. These values of a and b combine with (12) to determine $\Delta\tau_d$, and then $\Delta\tau$ is determined by (13). Since a and b depend upon U, which changes during the iteration, we recompute the values of a and b every 25 iterations as well as at the beginning of each time step.

4. TEST CALCULATIONS

The method embodied in equations (8) and (9) has been used to solve two different unsteady two-dimensional test problems, a conventional driven cavity and flow past a rectangular obstacle. Both problems were solved as true unsteady calculations, starting from initial conditions far away from the final steady state solution. The driven cavity problem was solved using two different spatial discretizations and both problems were solved for a wide range of Δt, varying from small values of the order of Δ/U to very large (essentially infinite) values. The total number of iterations, summed over all time steps in each calculation, is used as an overall measure of computational efficiency. These total iteration counts therefore represent averages over the transient history of the flow field as it evolves from highly unsteady initial conditions towards a steady state. For each grid and Δt, approximate optimal values of α and β were empirically determined by searching in increments of $\Delta\alpha = 0{\cdot}25$ and $\Delta\beta = 0{\cdot}1$ for the values that minimized the iteration counts and the resulting 'best' iteration counts

were recorded. Compromise Δt-independent values of α and β were also determined and the corresponding 'compromise' iteration counts were usually found to be within 25% of the best iteration counts. In order to assess the benefits of our new expressions for a and b, comparison calculations were also performed using the conventional values $a = \alpha U$ and $b = 0$ (using the compromise value for α) and the resulting 'conventional' iteration counts were compared with the compromise iteration counts. Speed-up factors are defined as the ratios of conventional to compromise iteration counts. These speed-up factors are conservative; they would of course be larger if they were defined relative to the best rather than the compromise iteration counts. The time step safety factor f for each calculation was simply set to the largest multiple of 0·05 for which convergence occurred.

The driven cavity problem is a simulation of flow in a unit square, the lid or top boundary of which slides parallel to itself at unit velocity. The Reynolds number based on lid velocity and side length is $Re = 400$. The fluid is initially quiescent and the motion is started impulsively at $t = 0$. Unsteady calculations are run out to a time $t = 25$, where the solution has become nearly steady, while true steady solutions are computed by setting Δt to a very large value. Calculations were performed for various values of Δt using two different spatial meshes, a coarse 10×10 mesh ($\Delta x = \Delta y = 0{\cdot}1$) and a finer 40×40 mesh ($\Delta x = \Delta y = 0{\cdot}025$). The steady state velocity vectors for the 40×40 case are shown in Figure 1. Iteration counts and speed-up factors are given in Table I for the 10×10 case and in Table II for the 40×40 case. The tables also show the best and compromise values of α and β and the corresponding compromise and conventional values of a and b at iteration convergence.

Inspection of the tables shows several clear trends and leads to some definite conclusions. In the 10×10 case summarized in Table I we see clear differences in behaviour between small and large values of Δt. For $\Delta t \geqslant 1$ our new values of a are essentially the same as the conventional ones, and the modest speed-up factors that we obtain are due to the additional damping provided by b. For $\Delta t \leqslant 1$, however, the situation is entirely different; b goes to zero, indicating that additional damping is

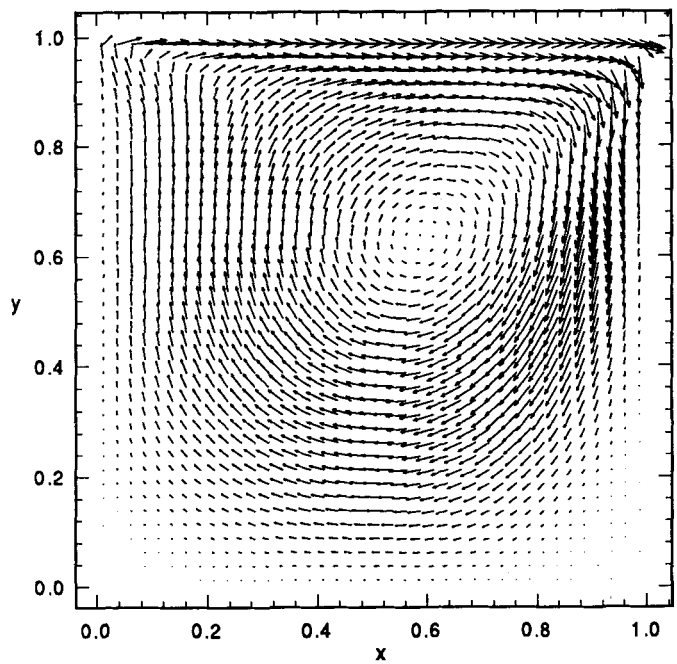

Figure 1. Steady state velocity vectors for 40 × 40 driven cavity problem

Table I. Performance data for 10×10 driven cavity with $Re = 400$

	Best empirical values			Compromise $\alpha = 1$, $\beta = 0{\cdot}5$			Conventional $a = U$, $b = 0$		Speed-up factor
Δt	α	β	Iter.	a	b	Iter.	a	Iter.	
10^{10}	0·25	0·4	641	1·00	0·0329	721	1·00	1397	1·9
25	0·25	0·3	569	1·00	0·0308	679	1·00	1138	1·7
5	0·5	0·3	1233	1·00	0·0227	1477	1·00	1760	1·2
1	0·5	0·8	1721	1·01	0·0	2116	1·00	2109	1·0
0·5	0·5	$b = 0$	1913	1·03	0·0	2252	1·00	2254	1·0
0·1	1·25	$b = 0$	3765	1·51	0·0	4244	1·00	6187	1·5
0·05	1·75	$b = 0$	5098	2·47	0·0	6317	1·00	17208	2·7

Table II. Performance data for 40×40 driven cavity with $Re = 400$

	Best empirical values			Compromise $\alpha = 1{\cdot}25$, $\beta = 0{\cdot}5$			Conventional $a = 1{\cdot}25U$, $b = 0$		Speed-up factor
Δt	α	β	Iter.	a	b	Iter.	a	Iter.	
10^{10}	0·25	0·3	6171	1·25	0·0063	6647	125	6665	1·0
25	0·25	0·4	4696	1·25	0·0043	5162	125	5117	1·0
5	0·5	0·8	9143	1·25	0·0	9685	1·25	9685	1·0
1	0·5	$b = 0$	13563	1·26	0·0	13687	1·25	13725	1·0
0·5	0·5	$b = 0$	15412	1·28	0·0	15522	1·25	15580	1·0
0·1	1·25	$b = 0$	23273	1·89	0·0	23273	1·25	33635	1·5
0·05	1·75	$b = 0$	29275	3·09	0·0	30873	1·25	76495	2·5
0·02	1·25	$b = 0$	46931	7·15	0·0	46931	1·25	240752	5·0
0·01	0·75	$b = 0$	68769	14·13	0·0	78792	1·25	543425	7·0

no longer beneficial, while our new values of a become substantially larger than conventional values. These larger values of a produce significant speed-up factors, approaching a value of three for small Δt.

The 40×40 case summarized in Table II exhibits generally similar behaviour, except that we now obtain no appreciable benefits from b even for large Δt. A similar reduction in the benefits of damping on finer grids was previously observed by Ramshaw and Mousseau[11] in the analogous scheme for steady state calculations. Here, however, we obtain even greater benefits from the larger values of a for small Δt, where speed-up factors as large as seven are obtained.

Our second test problem is a simulation of flow past a rectangular obstacle. The computational region is a rectangle of length $L_x = 2$ and width $L_y = 1$, subdivided by a uniform 40×20 computational mesh with $\Delta x = \Delta y = 0{\cdot}05$. The flow enters the region through the left boundary, flows past the obstacle and exits through the right boundary. The top and bottom boundaries are solid walls at which free slip boundary conditions are imposed on the velocity. The obstacle has a length of 0·2 in the streamwise direction and a width of 0·3 in the transverse direction and is placed symmetrically between the top and bottom boundaries, with the left edge of the obstacle located at $x = 0{\cdot}25$. No-slip velocity boundary conditions are imposed on the obstacle surface. The inlet flow is uniform with a streamwise velocity $u = 0{\cdot}027$ and a transverse velocity $v = 0$, which values were also used as initial conditions at $t = 0$. The Reynolds number based on inlet velocity and obstacle width is $Re = 50$, which is low enough that vortex shedding does not occur and true steady solutions can be obtained. At the outflow boundary the pressure is set to zero and the streamwise gradients of u and v are also required to vanish.

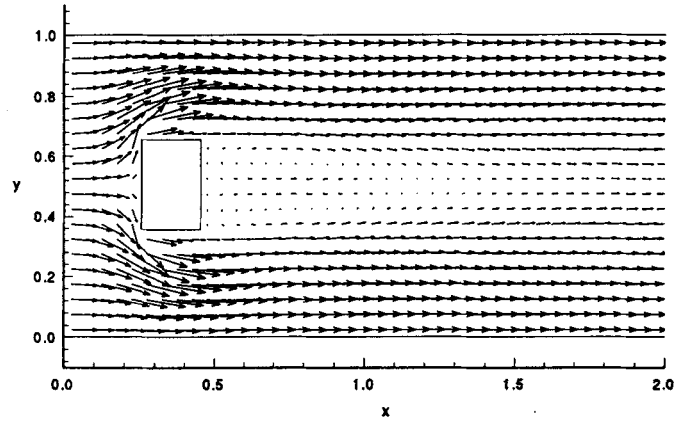

Figure 2. Steady state velocity vectors for 40 × 20 obstacle problem

Table III. Performance data for 40 × 20 obstacle problem with $Re = 50$

	Best empirical values			Compromise $\alpha = 2{\cdot}5$, $\beta = 0{\cdot}5$			Conventional $a = 2{\cdot}5U$, $b = 0$		
Δt	α	β	Iter.	a	b	Iter.	a	Iter.	Speed-up factor
10^{10}	0·25	0·2	1465	0·12	0·0005	2460	0·12	2457	1·0
150	1·0	$b = 0$	1347	0·12	0·0	1927	0·12	1927	1·0
50	1·0	$b = 0$	2872	0·12	0·0	3338	0·12	3339	1·0
25	1·25	$b = 0$	3971	0·12	0·0	4550	0·12	4550	1·0
10	2·0	$b = 0$	5755	0·12	0·0	6374	0·12	6408	1·0
5	4·25	$b = 0$	8598	0·14	0·0	11236	0·12	14790	1·3
1	5·0	$b = 0$	23792	0·38	0·0	39349	0·12	141098	3·6
0·5	3·75	$b = 0$	33931	0·72	0·0	42326	0·12	301492	7·1

Unsteady calculations are run out to a time $t = 150$, where the solution has become nearly steady, while true steady solutions are computed by setting Δt to a very large value. Calculations were performed using various different values of Δt. The resulting steady state velocity vectors are plotted in Figure 2, which shows that a recirculation region has formed behind the obstacle.

The performance data for this test problem are shown in Table III. In this problem the compromise values of b resulted in no speed-up relative to the conventional value $b = 0$. (Indeed, the best value for b was non-zero only in the steady state case.) However, the use of larger values of a for smaller Δt again produced very significant speed-up factors, becoming larger than seven for the smallest time step considered ($\Delta t = 0{\cdot}5$).

5. CONCLUDING REMARKS

We have presented a new artificial compressibility iteration scheme for solving the coupled non-linear algebraic equations resulting from implicit time discretizations of the unsteady incompressible Navier–Stokes equations. We have found that the rate of convergence may be significantly accelerated, relative to conventional schemes of this type, by a suitable choice of the parameters a and b. For large Δt the fastest convergence is obtained by using conventional values of a ($a \sim |\mathbf{u}|$) in conjunction with

relatively large values of the new parameter b. In contrast, the fastest convergence for small Δt is obtained by setting $b = 0$ and letting a be much larger than conventional values. This somewhat counter-intuitive behaviour has been interpreted in terms of the wave propagation and damping characteristics of the scheme. A heuristic Fourier convergence rate analysis has been used to propose simple analytical expressions for a and b, which provide reasonable estimates of their optimal values as functions of Δt. The use of these expressions removes or greatly reduces the need to determine optimal values of a and b through a tedious trial-and-error process, which would otherwise be necessary.

It seems likely that modest further improvements in convergence rate might be obtained by additional refinements of the method, particularly in more complicated problems involving non-uniform meshes with large variations in cell size. In such problems it may be advantageous to allow different values of a, b and $\Delta\tau$ in different cells of the mesh. It would also be of interest to perform numerical experiments with the method using unstructured meshes, finite element methods and spectral methods.

The present scheme preserves the simplicity and clear physical interpretation of earlier artificial compressibility methods and these attributes are its main advantage. However, one pays a price for this simplicity in terms of computational efficiency: even with its accelerated convergence, the present scheme is considerably less efficient than more sophisticated schemes. The development of such schemes has received much attention during recent years and substantial progress has been made. We mention in particular an evolving family of inexact Newton–Krylov schemes which is producing excellent results in a variety of fluid dynamics and plasma physics applications.[18–23] These schemes are achieving impressive levels of performance but are considerably more complex and less friendly than simple schemes of the present type. Thus the present scheme is not intended to compete with these more sophisticated schemes in terms of computational efficiency. Its role is rather to provide an admittedly less efficient but much simpler alternative scheme which is much quicker and easier to implement and modify. The present scheme may therefore be suitable for practical applications in situations where simplicity, friendliness and development time take priority over execution time. We are also hopeful that the simplicity and clear physical interpretation of the method will make it useful for educational purposes.

ACKNOWLEDGEMENTS

We are grateful to G. L. Mesina, V. A. Mousseau and V. H. Ransom for helpful discussions.

This work was performed under the auspices of the U.S. Department of Energy under DOE Field Office, Idaho Contract DE-AC07-94ID13223, supported in part by the INEL Long-Term Research Initiative in Computational Mechanics.

REFERENCES

1. A. J. Chorin, 'A numerical method for solving incompressible viscous flow problems', *J. Comput. Phys.*, **2**, 12–26 (1967).
2. D. Choi and C. L. Merkle, 'Application of time-iterative schemes to incompressible flow', *AIAA J.*, **23**, 1518–1524 (1985).
3. E. Turkel, 'Preconditioned methods for solving the incompressible and low speed compressible equations', *J. Comput. Phys.*, **72**, 277–298 (1987).
4. S. E. Rogers, D. Kwak and U. Kaul, 'On the accuracy of the pseudocompressibility method in solving the incompressible Navier–Stokes equations', *Appl. Math. Modell.*, **11**, 35–44 (1987).
5. W. R. Briley, R. C. Buggeln and H. McDonald, 'Solution of the incompressible Navier–Stokes equations using artificial compressibility methods', in D. L. Dwoyer, M. Y. Hussaini and R. B. Voigt (eds), *Lecture Notes in Physics*, Vol. 323, Springer, Berlin, 1989, pp. 156–160.
6. R. Peyret, 'Unsteady evolution of a horizontal jet in a stratified fluid', *J. Fluid Mech.*, **78**, 49–63 (1976).
7. R. Peyret and T. D. Taylor, *Computational Methods for Fluid Flow*, Springer, New York, 1983.
8. C. L. Merkle and M. Athavale, 'Time-accurate unsteady incompressible flow algorithms based on artificial compressibility', *AIAA Paper 87-1137*, 1987.

9. W. Y. Soh and J. W. Goodrich, 'Unsteady solution of incompressible Navier–Stokes equations', *J. Comput. Phys.*, **79**, 113–134 (1988).
10. S. E. Rogers and D. Kwak, 'Upwind differencing scheme for the time-accurate incompressible Navier–Stokes equations', *AIAA J.*, **28**, 253–262 (1990).
11. J. D. Ramshaw and V. A. Mousseau, 'Accelerated artificial compressibility method for steady-state incompressible flow calculations', *Comput. Fluids*, **18**, 361–367 (1990).
12. J. D. Ramshaw and G. L. Mesina, 'A hybrid penalty– pseudocompressibility method for transient incompressible fluid flow', *Comput. Fluids*, **20**, 165–175 (1991).
13. J. D. Ramshaw and V. A. Mousseau, 'Damped artificial compressibility method for steady-state low-speed flow calculations', *Comput. Fluids*, **20**, 177–186 (1991).
14. T. F. Chan and H. C. Elman, 'Fourier analysis of iterative methods for elliptic problems', *SIAM Rev.*, **31**, 20–49 (1989).
15. T. F. Chan, 'Fourier analysis of relaxed incomplete factorization preconditioners', *SIAM J. Sci. Stat. Comput.*, **12**, 668–680 (1991).
16. J. D. Ramshaw and G. L. Mesina, 'Simplified heuristic Fourier analysis of iteration convergence rates', *Commun. Numer. Methods, Engn.*, **10**, 481–487 (1994).
17. P. J. Roache, *Computational Fluid Dynamics*, Hermosa, Albuquerque, NM, 1972, p. 85.
18. P. Chin *et al.*, 'Preconditioned conjugate gradient methods for the incompressible Navier–Stokes equations', *Int. J. numer. methods fluids*, **15**, 273–295 (1992).
19. P. N. Brown and Y. Saad, 'Hybrid Krylov methods for nonlinear systems of equations', *SIAM J. Sci. Stat. Comput.*, **11**, 450–481 (1990).
20. D. A. Knoll and P. R. McHugh, 'NEWEDGE: a 2-D fully implicit edge plasma fluid code for advanced physics and complex geometries', *J. Nucl. Mater.*, **196–198**, 352–356 (1992).
21. D. A. Knoll and P. R. McHugh, 'A fully implicit direct Newton solver for the Navier–Stokes equations', *Int. J. numer. methods fluids*, **17**, 449–461 (1993).
22. D. A. Knoll and P. R. McHugh, 'An inexact Newton algorithm for the tokamak edge plasma fluid equations on a multiply connected domain', *J. Comput. Phys.*, **116**, 281–291 (1995).
23. P. R. McHugh and D. A. Knoll, 'Fully coupled finite volume solutions of the incompressible Navier–Stokes and energy equations using inexact Newton method', *Int. J. numer. methods fluids*, **19**, 439–455 (1994).